CrossMark

Preparation and characterization of nanocrystalline praseodymium oxide via a simple precipitation approach

Sahar Zinatloo-Ajabshir[1] · Masoud Salavati-Niasari[1,2]

Abstract Pr_6O_{11} nanostructures were successfully prepared by new facile precipitation strategies that employed $Pr(NO_3)_3 \cdot 6H_2O$ and a novel precipitating agent in presence of poly ethylene glycol (PEG) as starting materials, and water as the solvent. The novelty of this study is the application of tetramethylethylenediamine (TMED) as a new precipitating and co-capping agent in presence of PEG for the synthesis of praseodymium oxide nanostructures. The formation of as-produced nanostructures and their structure, shape and elemental composition were analyzed by means of several techniques including FT-IR, EDAX, XRD, TEM and FESEM. The optical properties of the samples were characterized by (UV–Vis) absorption and (PL) spectroscopy. In addition, the photocatalyst activity of as-prepared Pr_6O_{11} nanostructures was evaluated by degradation of 2-naphthol under ultraviolet light irradiation. Based on the experimental findings in this work, it was found that particle size and shape of the final praseodymium oxide could be dramatically affected via the dosage of TMED. Furthermore, the mechanism effect of TMED in presence of PEG for formation of nanostructures discussed preliminarily.

1 Introduction

Praseodymium oxide, which belongs to the class of rare earth metal oxides, has been widely used in promoters and stabilizers in combustion catalysts, pigments, materials with higher electrical conductivity, catalysts, and oxygen-storage components due to its specific and excellent optical and electrical properties [1–5]. It is reported that praseodymium oxide forms a homologous series with a number of stoichiometrically defined oxides: Pr_nO_{2n-2}, with n = 4, 7, 9, 10, 11, 12,… Pr_6O_{11} is well known as the most attractive, stable and steadiest form of these oxides at ambient temperature and pressure [6]. So far, very limited numbers synthetic methods have been developed for the fabrication of nanostructured praseodymium oxide such as electrospinning [7], molten salt [8], thermal decomposition [9], hydrothermal [10], electrochemical [11], and precipitation [6]. The introduction of the reproducible, effective and simple approach to synthesize nanostructured praseodymium oxide is important to the potential examinations of its characteristics. It is generally accepted that the properties of nanostructured materials could be extremely affected by their shape and particle size [12–15]. So, presenting appropriate methods to synthesize Pr_6O_{11} and controlling its morphology and particle size seems required and important.

The present work describes a facile precipitation method to prepare nanostructures of praseodymium oxide with the aid of tetramethylethylenediamine (TMED) as novel precipitating and co-capping agent in presence of PEG. Many inorganic nanostructured materials have been synthesized by the precipitation approach as a suitable synthetic process. This approach is well known as simple, cost effective, reproducible, convenient and reliable synthetic approach and provides promising and effective way to the preparation of

✉ Masoud Salavati-Niasari
salavati@kashanu.ac.ir

1 Institute of Nano Science and Nano Technology, University of Kashan, P.O. Box 87317-51167, Kashan, I.R. Iran

2 Department of Inorganic Chemistry, Faculty of Chemistry, University of Kashan, P.O. Box 87317-51167, Kashan, I.R. Iran

Tetramethylethylenediamine with high hindrance in the presence of PEG has a role of co-capping agent for the Pr(OH)₃ nanoparticle
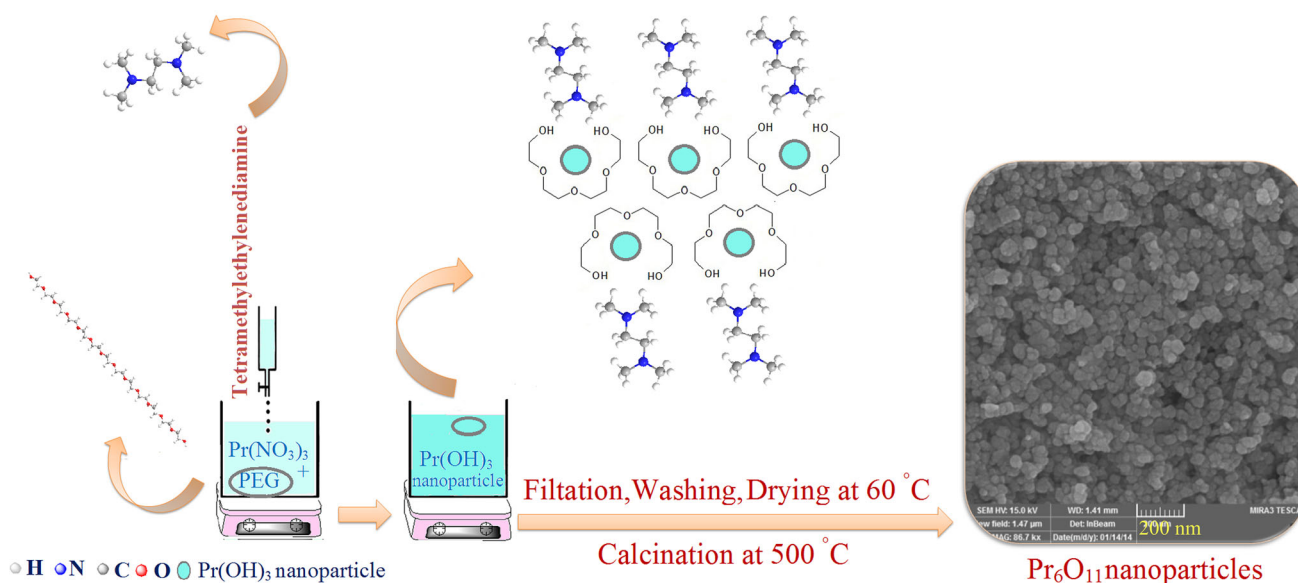
Scheme 1 Schematic diagram of the synthesis of praseodymium oxide nanoparticles

homogeneous and uniform nanomaterials. To our knowledge, it is the first time that TMED is applied as precipitating and co-capping agent for the preparation of Pr_6O_{11} nanostructures and the effect of its dosage on the shape and particle size of praseodymium oxide through a precipitation approach in the presence of PEG is examined. Furthermore, the optical characteristics of the products were characterized by (UV–Vis) absorption and (PL) spectroscopy. The photocatalyst activity of the as-produced praseodymium oxide nanostructures was studied by degradation of 2-naphthol under ultraviolet light irradiation.

2 Experimental

2.1 Materials

Pr_6O_{11} nanostructures were synthesized, utilizing the following chemical reagents, purchased from Merck Company and used as received: praseodymium nitrate $(Pr(NO_3)_3 \cdot 6H_2O)$ (PN), poly ethylene glycol 600 (PEG 600), TMED and liquor ammonia solution containing 25 % ammonia.
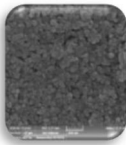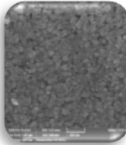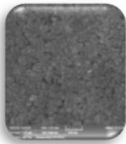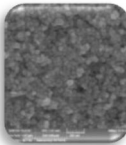
2.2 Synthesis of Pr_6O_{11} nanostructures
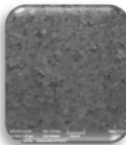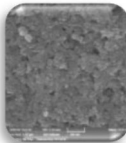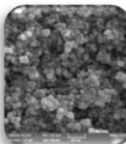
Pr_6O_{11} nanoparticles (PNPs) were prepared by simple precipitation approach. In a typical experiment, 0.085 ml $(5.75 \times 10^{-4}$ mol) of TMED was dissolved in 20 ml of

distilled water and then was added drop-wise to 20 ml solution containing 0.25 g $(5.75 \times 10^{-4}$ mol) of praseodymium nitrate and stoichiometric amount of PEG under magnetic stirring for 10 min. The green precipitate was centrifuged, washed out three times with distilled water, dried at 60 °C and calcined at 500 °C for 3 h (sample no. 1). Schematic diagram of the synthetic pathway of PNPs is illustrated in Scheme 1. The experiment was carried out by applying 0.17, 0.26, 0.34, and 0.43 ml of TMED at the identical conditions, respectively. To study the effect of TMED, a blank test was performed by NH_4OH instead of TMED. In the blank test, 0.65 ml $(46 \times 10^{-4}$ mol) of NH_4OH dissolved in 20 ml distilled water and was added into a solution including 0.25 g $(5.75 \times 10^{-4}$ mol) of praseodymium nitrate and stoichiometric amount of PEG dissolved in 20 ml of distilled water. For comparison, one experiment was performed without using any PEG and named as blank test1. A list of preparation conditions and morphologies of the samples no. 1–7 is presented in Table 1. The detailed morphological, structural and optical properties of the as-synthesized products were characterized by using EDS, TEM, XRD, SEM, FT-IR, PL and UV–Vis.

2.3 Characterization

FESEM images of samples were visualized by a Tescan mira3 field emission scanning electron microscope (FESEM). Fourier transform infrared spectra were obtained

Table 1 Preparation conditions for Pr_6O_{11} samples

| Sample No.	Precipitating agent	Dosage of precipitator (ml)	Capping agent	SEM
1	TMED	0.085	PEG	
2	TMED	0.17	PEG	
3	TMED	0.26	PEG	
4	TMED	0.34	PEG	
5	TMED	0.43	PEG	
6[a]	TMED	0.34	–	
7[b]	NH$_4$OH	0.65	PEG	

[a] Blank test, in the absence of PEG

[b] Blank test1, in the absence of TMED

on a Shimadzu Varian 4300 spectrophotometer in KBr pellets in the 400–4000 cm^{-1} range. The EDS analysis was done by a Philips XL30 microscope. The electronic spectra of the as-prepared PNPs were obtained on a Scinco UV–Vis scanning spectrometer (Model S-4100). Transmission electron microscope (TEM) images of PNPs were taken on a JEM-2100 with an accelerating voltage of 200 kV. A Perkin Elmer (LS 55) fluorescence spectrophotometer was applied to perform room temperature photoluminescence (PL) analysis. Powder X-ray diffraction (XRD) patterns were recorded by a diffractometer of Philips

Company with X'PertPromonochromatized Cu Kα radiation ($\lambda = 1.54$ Å, operated on 35 mA and 40 kV current).

2.4 Photocatalytic test

The photocatalytic activity of PNPs obtained from sample no.4 was evaluated by the degradation of 2-naphthol solution as a target pollutant. A quartz photocatalytic reactor was used to perform the degradation reaction. The photocatalytic degradation was carried out by using 0.0012 g of
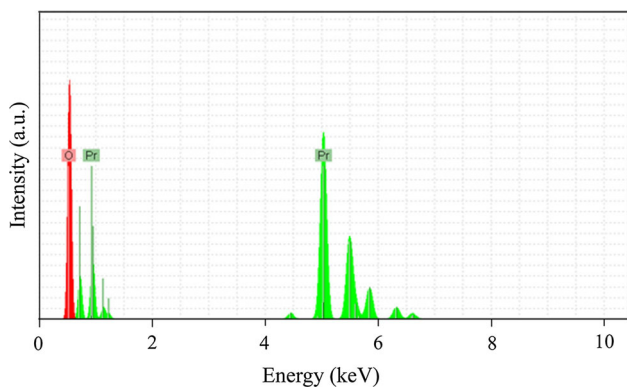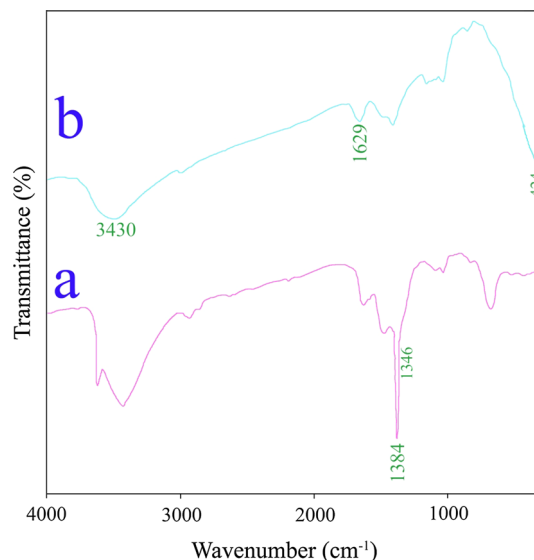
Fig. 1 EDS pattern of Pr_6O_{11} (sample no. 4)
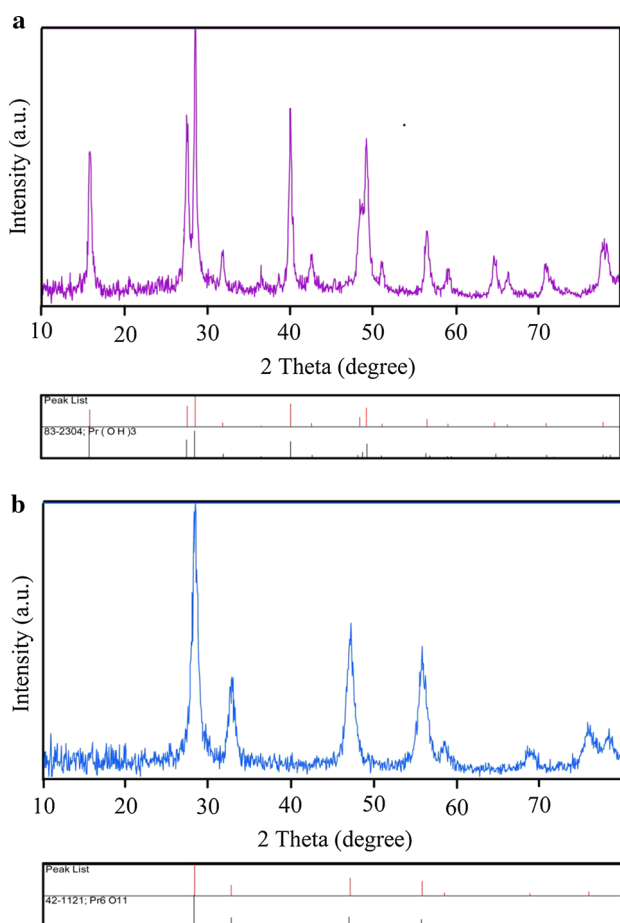
Fig. 2 XRD patterns of sample no. 4 after washing (**a**), and after calcinacion (**b**)

Fig. 3 FT-IR spectra of sample no. 4 after washing (*a*), and after calcinacion (*b*)

inside a black box that equipped with a fan. Aliquots of the mixture were taken at definite interval of times during the irradiation, and after centrifugation they were analyzed by a UV–Vis spectrometer. The 2-naphthol degradation efficiency was calculated as follow:
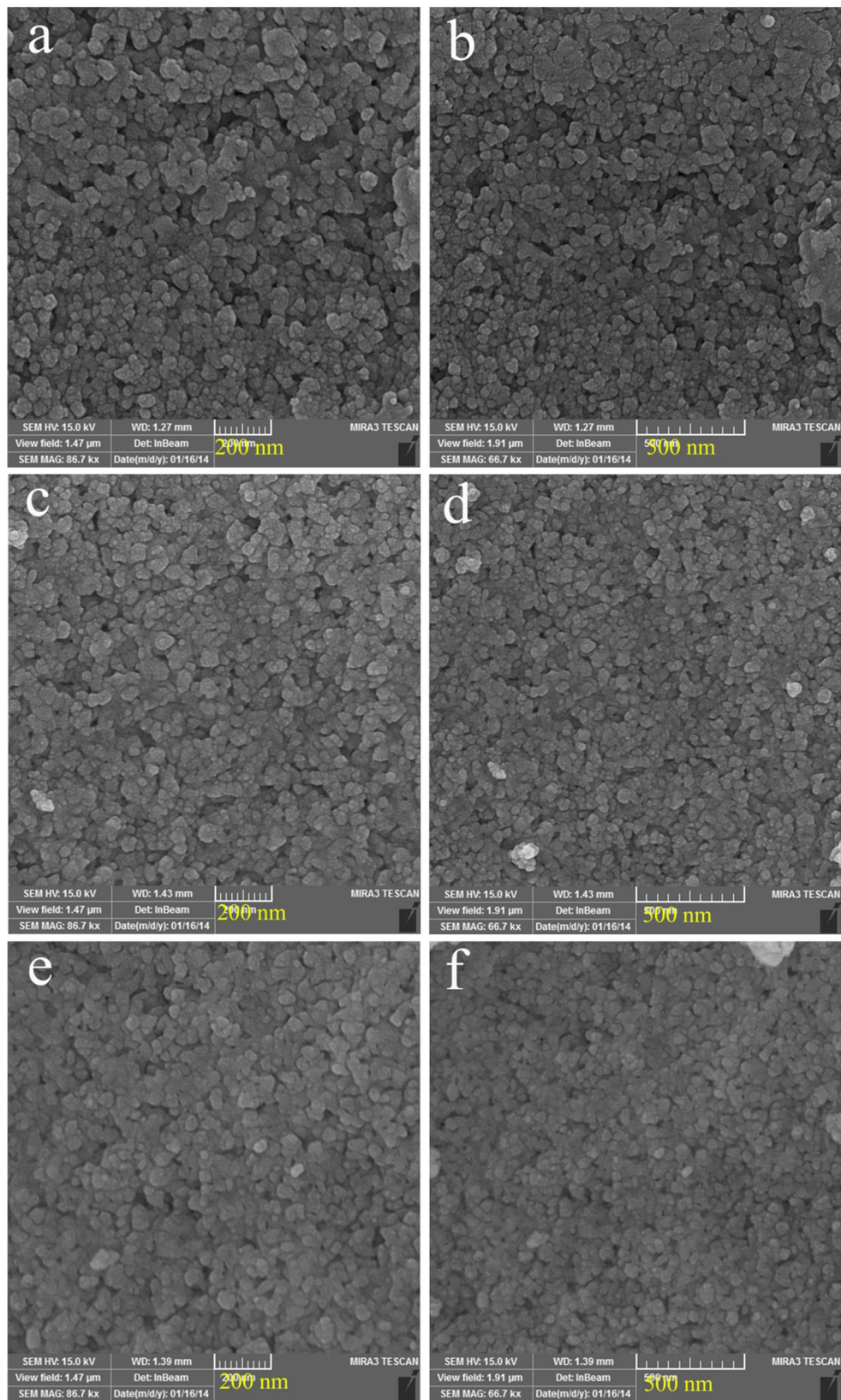
$$(\%) = \frac{C_0 - C_t}{C_0} \times 100 \tag{1}$$

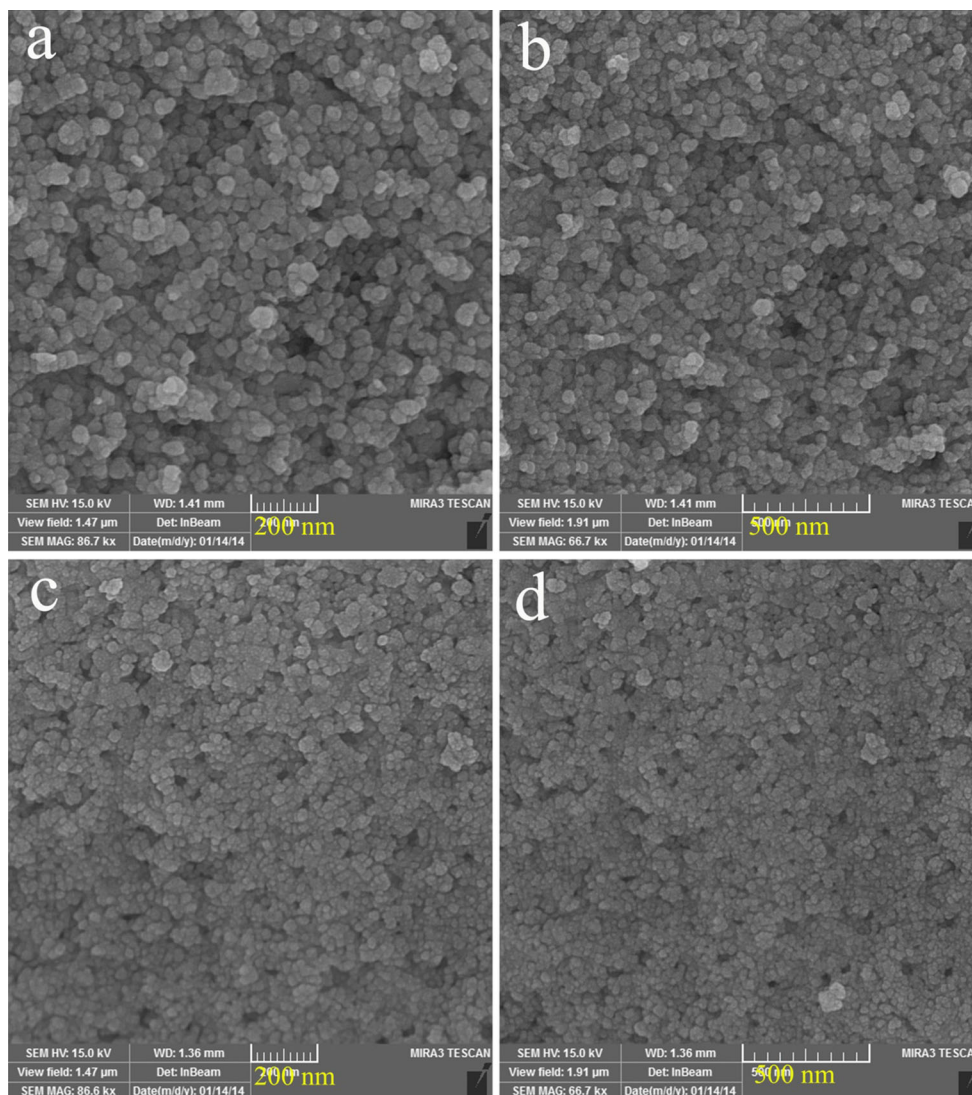where C_t and C_0 are the concentration of 2-naphthol at t and 0 min, respectively.

3 Results and discussion

The chemical composition and purity of as-prepared PNPs was examined by EDS analysis (Fig. 1). The EDX pattern of PNPs (sample no. 4) in Fig. 1 shows that the only elements which existed were Pr and O elements. Moreover, no impurity peaks are exhibited, which confirms a high level of purity in these PNPs.

The crystal structure, average crystallite diameter characterization of the PNPs was done by Powder XRD analysis. XRD patterns of the sample no. 4 after washing steps, and after calcination are illustrated in Fig. 2. All of reflection peaks in Fig. 2a can be attributed to pure hexagonal $Pr(OH)_3$ (space group P63/m, JCPDS card 83-2304). All the diffraction peaks of PNPs in Fig. 2b are well-matched to pure cubic Pr_6O_{11} with Fm3 m space group (JCPDS 42-1121). No impurities can be found in this pattern, revealing that a pure Pr_6O_{11} has been obtained. From XRD data in Fig. 2b, the mean crystallite size (D_C) of the as-synthesized PNPs, sample no. 4, was estimated to

2-naphthol solution including 0.05 g of PNPs at room temperature. To reach adsorption equilibrium, this mixture was aerated for 30 min. Later, the mixture was placed inside the photoreactor in which the vessel was 40 cm away from the UV source of 400 W mercury lamps. To hinder UV leakage, the light source and quartz vessel were placed

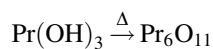**Fig. 4** SEM images of **a**, **b** sample no. 1, **c**, **d** sample no. 2, and **e**, **f** sample no. 3
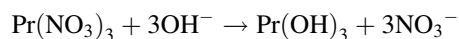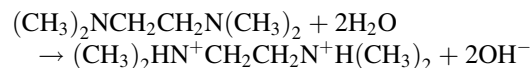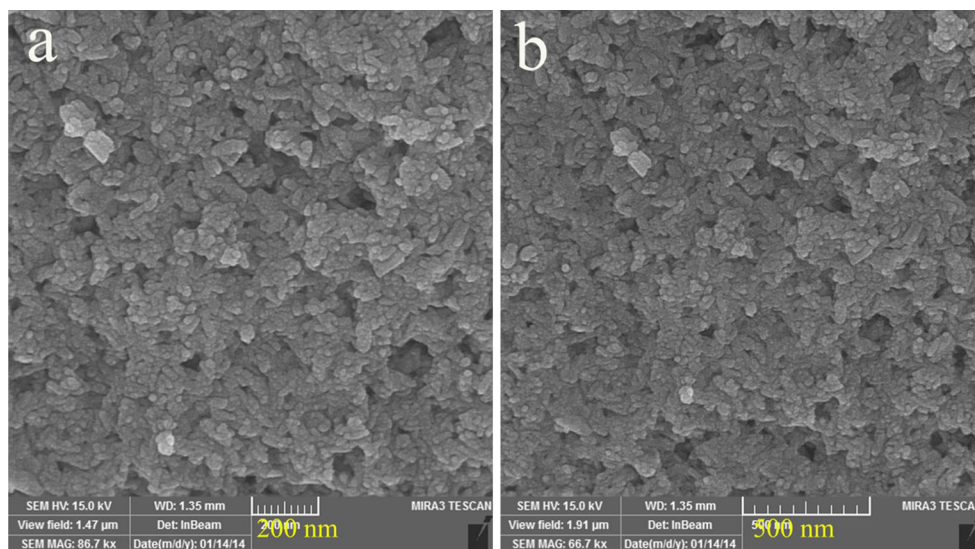
Fig. 5 SEM images of **a**, **b** sample no. 4, and **c**, **d** sample no. 5

be 23 nm using the Scherrer equation, $D_C = 0.94\lambda/\beta\cos\Theta$ [16], Θ is the diffraction angle, β is the breadth of the observed diffraction line at its half intensity maximum, and λ is the wavelength of X-ray source applied in XRD.
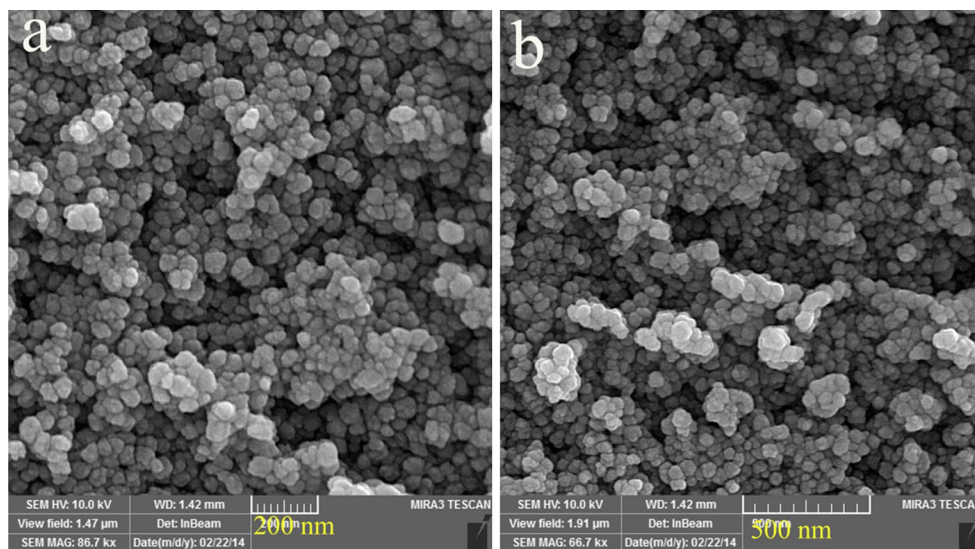
To investigate the surface of sample no. 4 after washing steps and after calcination, FTIR spectroscopy was applied. FT-IR spectra are seen in Fig. 3. The spectrum of sample after washing steps shows the (C–H) bending vibration band located at 1384 cm^{-1} and (C–N) stretching vibration band at 1346 cm^{-1} due to the presence of TMED (Fig. 3a). They completely vanish after calcination at 500 $^\circ$C. In the case PNPs, the absorption band centered at 3430 cm^{-1} and a weak peak at 1629 cm^{-1} are related to the v(OH) stretching and bending vibrations of surface adsorbed water molecules, respectively [17]. The characteristic band of praseodymium oxide observed at 424 cm^{-1} is assigned to Pr–O vibration [18] (Fig. 3b).

The novelty of this study compared to other research is that for the preparation of Pr$_6$O$_{11}$, TMED as a new precipitating agent in presence of PEG was applied. TMED can precipitate Pr(OH)$_3$ from Pr(NO$_3$)$_3$. Moreover, TMED has high steric hindrance and can play co-capping agent role to control shape and size of the Pr(OH)$_3$ nanoparticles in the presence of PEG by hindering the aggregation of nanoparticles. It seems that TMED in the presence of PEG causes nucleation occurrence rather than the growth of particle (Scheme 1). The possible formation mechanism of PNPs utilizing TMED in the presence of PEG can be assumed as:

$$(CH_3)_2NCH_2CH_2N(CH_3)_2 + 2H_2O$$
$$\rightarrow (CH_3)_2HN^+CH_2CH_2N^+H(CH_3)_2 + 2OH^-$$

$$Pr(NO_3)_3 + 3OH^- \rightarrow Pr(OH)_3 + 3NO_3^-$$

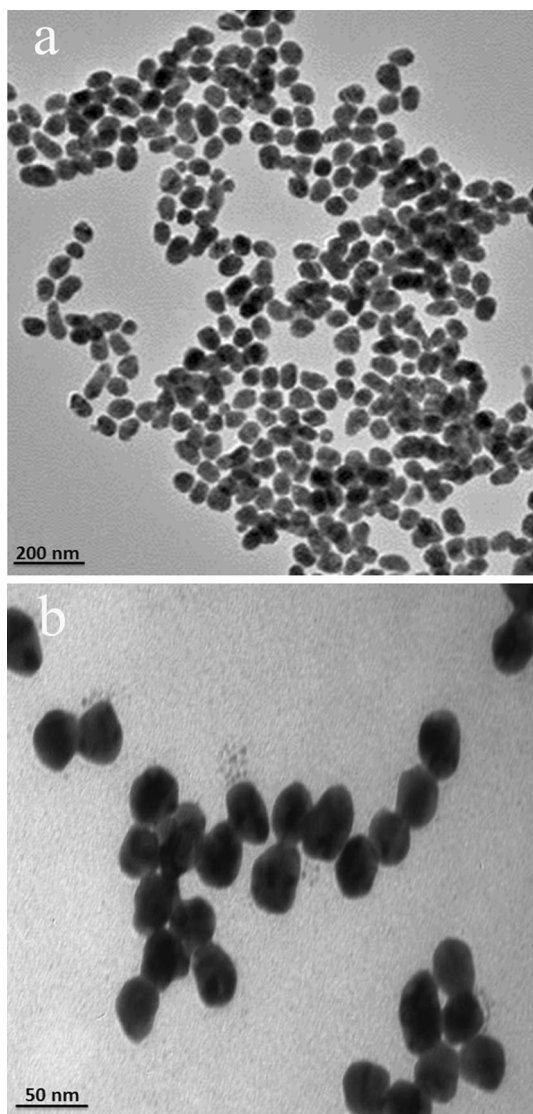$$Pr(OH)_3 \xrightarrow{\Delta} Pr_6O_{11}$$

Fig. 6 SEM images of sample no. 6

Fig. 7 SEM images of the sample no. 7

To investigate the influence of TMED dosage on the shape of the Pr_6O_{11} in the presence of PEG, SEM images of samples with 0.085, 0.17, 0.26, 0.34, and 0.43 ml of TMED were taken and illustrated in Figs. 4 and 5, respectively. As shown in Figs. 4a–f and 5a, b, by increasing the dosage of TMED from 0.085 to 0.34 ml, the amount of uniform and spherical PNPs increased. When the dosage of TMED was 0.34 ml, very uniform sphere-like PNPs with small grain size were obtained (sample no. 4). It seems that when dosage of TMED increases, the chance of collision between $Pr(OH)_3$ nanoparticles decreases due to steric hindrance effect of TMED. Although with more dosage of TMED (0.43 ml), nanoparticles with sphere-like shape can

be formed, these particles were not uniform and were high aggregated in some places (Fig. 5c, d). These results indicated that the dosage of TMED in the presence of PEG has a great impact on the particle size and shape control of praseodymium oxide samples.

To study the influence of the presence of PEG on the shape of the PNPs, sample no. 6 was synthesized as blank sample without applying any PEG. SEM image of sample no. 6 is exhibited in Fig. 6a, b. It is noteworthy that irregular and uninformed agglomerated praseodymium oxide particles with large grain size were obtained. It is clearly observed that PEG600 plays an effective role to control the size of the $Pr(OH)_3$ nanoparticles and hinders the further
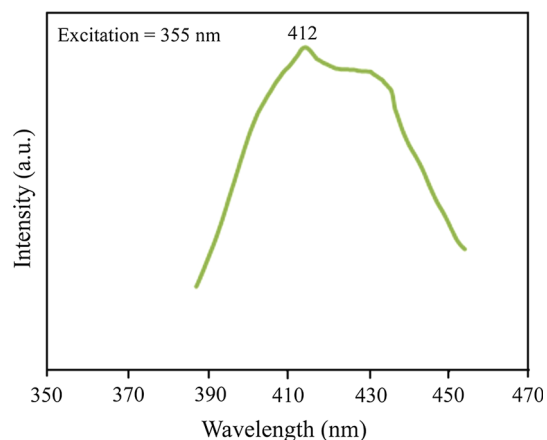
Fig. 8 TEM images of sample no. 4

Fig. 9 UV–Vis absorbance spectrum (**a**) of the sample no. 4 and plot to determine the band gap of Pr_6O_{11} (**b**)

Fig. 10 PL spectrum of the sample no. 4

aggregation of nanoparticles. PEG600 acts as a capping agent and has a great impact on the preparation of very uniform sphere-like PNPs (Fig. 5a, b). It has been approved that polymeric molecules of PEG are adsorbed preferentially on the nuclei surface to inhibit aggregation by steric hindrance mechanism [19]. So, an advantage of applying PEG is that it brings about to form very uniform sphere-like PNPs with small grain size.

To examine the influence of the TMED on the shape of the Pr_6O_{11}, sample no. 7 was prepared as blank test1 utilizing NH_4OH in the presence of PEG. SEM image of sample no. 7 is presented in Fig. 7a, b. SEM observations indicate that praseodymium oxide obtained from the sample no. 7 includes uninformed sphere-like particles with large grain size. These observations show that TMED play a key role in the formation of very uniform sphere-like

PNPs with small grain size. As already described, when TMED utilized as precipitating agent (Fig. 5a, b), the chance of collision between $Pr(OH)_3$ nanoparticles decreased due to steric hindrance influence of TMED, and therefore the size of nanoparticles decreased. These results indicate that TMED with high steric hindrance is a suitable
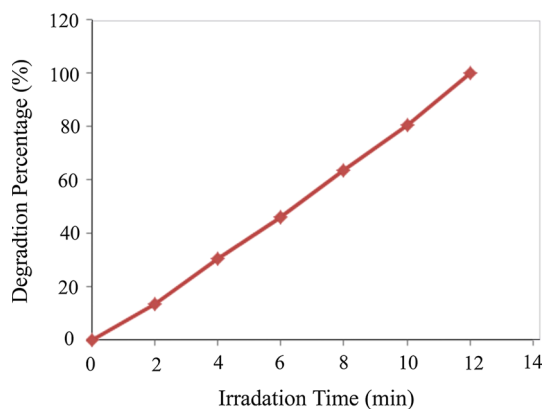
Fig. 11 Photocatalytic 2-naphthol degradation of praseodymium oxide nanostructures obtained from sample no. 4 under UV light

Scheme 2 Reaction mechanism of 2-naphthol photodegradation over PNPs under UV light irradiation

and favorable co-capping agent to control the size and shape of Pr_6O_{11}.

To characterize the detailed morphological characteristics of the as-prepared PNPs, TEM micrographs of the sample synthesized with the aid of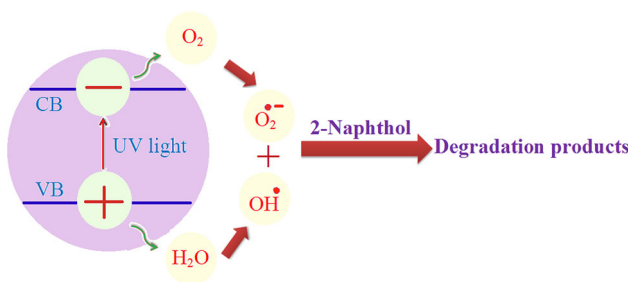 0.34 ml of TMED in the presence of PEG illustrated in Fig. 8a, b. The TEM images indicate that nanoparticles have a uniform spherical shape and narrow size distribution. Furthermore, the image shows that nanoparticles have diameters of 20–28 nm which is in a good agreement with those estimated particle size by XRD diffraction pattern.
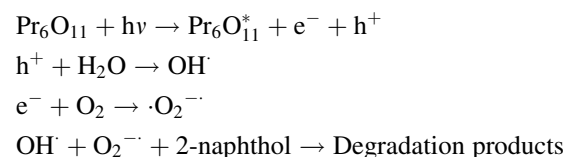
To assess the optical characteristics of the as-obtained PNPs, UV–Vis and PL spectra were recorded. Figure 9a shows the UV–Vis absorption spectrum of sample no. 4 (prepared by 0.34 ml of TMED in the presence of PEG). In the UV–Vis absorption spectrum, the absorption band was observed at 242 nm. The energy gap (Eg) can be evaluated based on the absorption spectrum using Tauc's relationship [20]:

$$(Ahv)^n = B(hv - E_g) \qquad (2)$$

where hv is the photon energy, A is absorbance amount, B is a material constant and n is 2 or 1/2 for direct and indirect transitions. The Eg for the absorption peak was obtained by extrapolating the linear portion of the plot of $(\alpha hv)^n$ curve against hv to zero (Fig. 9b). No linear relation was found for n = 1/2, suggesting that the as-synthesized PNPs is semiconductor with direct transition at this energy. The Eg value of the PNPs obtained to be 4.45 eV. The obtained results are in good agreement with previous reported investigation [21].

Figure 10 exhibits the PL spectrum of the sample no. 4. The excitation wavelength was 355 nm. An emission peak at around 412 nm can be observed in the PL spectrum. This emission peak is related to charge transition from the 4f band to the valence band of PNPs, which is similar to the previous literatures [21].

Photodegradation of 2-naphthol under UV light irradiation was employed to examine the photocatalytic activity of the as-prepared PNPs (sample no. 4). The obtained result is illustrated in Fig. 11. No 2-naphthol was practically broken down after 12 min without using UV light irradiation or PNPs. This observation indicated that the contribution of self-degradation was insignificant. The possible mechanism of the photocatalytic degradation of 2-naphthol can be assumed as:

$$Pr_6O_{11} + hv \rightarrow Pr_6O_{11}^* + e^- + h^+$$
$$h^+ + H_2O \rightarrow OH^.$$
$$e^- + O_2 \rightarrow \cdot O_2^{-.}$$
$$OH^. + O_2^{-.} + \text{2-naphthol} \rightarrow \text{Degradation products}$$

Table 2 Characterization comparison of Pr_6O_{11} nanostructures with other similar works

Method	Precursors	Size (nm)	Morphology	References
Precipitation method	$Pr(NO_3)_3 \cdot 6H_2O$, HMTA (needed boiling at 100 °C for 2 h)	>200 nm	Cylindrical shaped crystals	[4]
Precipitation route	Pr_6O_{11}, HNO_3, NaOH (needed aging for 16 h)	20–33 nm	Spherical nanoparticles with a significant amount of agglomeration	[6]
Precipitation method	$Pr(NO_3)_3 \cdot 6H_2O$, isopropanol and cyclohexane (as solvent), triethylamine	10–15 nm in diameter, 100–150 nm in length	Nanorods	[23]
Precipitation route	$PrCl_3 \cdot 7H_2O$, NaOH (needed aging for 3 days)	10–170 nm in length, 5–25 nm in width	Nanorods	[24]

Utilizing photocatalytic calculations by Eq. (1), the 2-naphthol degradation was about 100 % after 12 min irradiation of UV light. This result suggests that as-produced PNPs have high potential to be employed as an interesting candidate for photocatalytic applications under UV light irradiation. It is well known that the heterogeneous photocatalytic processes comprise diffusion, adsorption and reaction steps, and suitable distribution of the pore is effective and useful to diffusion of reactants and products, which prefer the photocatalytic reaction. In this research, the enhanced photocatalytic activity of the as-prepared PNPs can be assigned to favorable and appropriate distribution of the pore, high hydroxyl amount and high separation rate of charge carriers [22] (Scheme 2).

In comparison to other similar works, presented in Table 2, our approach is more facile, low-cost, low energy and time consumer and friendly to the environment. In this report, we presented a precipitation route to prepare praseodymium oxide with the aid of TMED in the presence of PEG and water as solvent in milder conditions and lower reaction times. The novelty of this study compared to other reports is that for the synthesis of praseodymium oxide, TMED as a new precipitating agent in presence of PEG was used. TMED with high steric hindrance in presence of PEG played either precipitating agent role and co-capping agent role in the water solvent. Results of this work indicate that the application of appropriate dosage of TMED in the presence of PEG led to synthesis of the products with high purity, very uniform spherical shapes and narrow size distributions.

4 Conclusions

This work presents a facile precipitation route to prepare very uniform sphere-like Pr_6O_{11} nanoparticles with small grain size with the aid of TMED and PEG. Applying of TMED both as a precipitating and co-capping agent in presence of PEG is the novelty of this investigation. The as-prepared Pr_6O_{11} nanoparticles can be used as an interesting candidate for photocatalytic applications under UV light irradiation in 2-naphthol elimination process from waste-water, since the 2-naphthol degradation percentage

was found to be 100 within 12 min. High purity of the as-obtained nanoparticles was proved by EDS, XRD, and FT-IR analyses. The optical properties of as-formed nanoparticles were also examined.

References

1. M. Kawabe, H. Ono, T. Sano, M. Tsuji, Y. Tamaura, Energy **22**, 1041 (1997)
2. P. Šulcová, J. Therm. Anal. Calorim. **82**, 51 (2005)
3. K. Asami, K. Kusakabe, N. Ashi, Y. Ohtsuka, Appl. Catal. A: Gen. **156**, 43 (1997)
4. S. Shrestha, C.M.Y. Yeung, C. Nunnerley, S.C. Tsang, Sens. Actuators, A **136**, 191 (2007)
5. S. Bernal, F.J. Botana, G. Cifredo, J.J. Calvino, A. Jobacho, J.M. Rodriguez-Izquierdo, J. Alloys Compd. **180**, 271 (1992)
6. B.M. Abu-Zied, Y.A. Mohamed, A.M. Asiri, J. Rare Earths **31**, 701 (2013)
7. M. Shamshi Hassan, Y.-S. Kang, B.-S. Kim, I.-S. Kim, H.-Y. Kim, M.-S. Khil, Superlattices Microstruct. **50**, 139 (2011)
8. X. Wang, J. Zhuang, Y. Li, J. Inorg. Chem. **5**, 946–948 (2004)
9. Basma A.A. Balboul, J. Anal. Appl. Pyrol. **88**, 192 (2010)
10. Y. Zhang, K. Han, X. Yin, Zh Fang, Zh Xu, W. Zhu, J. Cryst. Growth **311**, 3883 (2009)
11. X. Sun, T. Zhai, X. Lu, Sh Xie, P. Zhang, Ch. Wang, W. Zhao, P. Liu, Y. Tong, Mater. Res. Bull. **47**, 1783 (2012)
12. S. Zinatloo-Ajabshir, M. Salavati-Niasari, J. Ind. Eng. Chem. **20**, 3313 (2014)
13. F. Mohandes, M. Salavati-Niasari, RSC Adv. **4**, 25993 (2014)
14. S. Zinatloo-Ajabshir, M. Salavati-Niasari, Int. J. Appl. Ceram. Technol. **11**, 654 (2014)
15. F. Motahari, M.R. Mozdianfard, F. Soofivand, M. Salavati-Niasari, RSC Adv. **4**, 27654 (2014)
16. R.L. Snyder Jenkins, *Chemical Analysis: Introduction to X-ray Powder Diffractometry* (Wiley, New York, 1996), pp. 89–91
17. E. Esmaeili, M. Salavati-Niasari, F. Mohandes, F. Davar, H. Seyghalkar, Chem. Eng. Sci. **170**, 278 (2011)
18. M. Popa, M. Kakihana, Solid State Ion. **141–142**, 265 (2001)
19. A. Sobhani, M. Salavati-Niasari, Mater. Res. Bull. **53**, 7 (2014)
20. M. Salavati-Niasari, D. Ghanbari, M.R. Loghman-Estarki, Polyhedron **35**, 149 (2012)
21. N. Krishna Chandar, R. Jayavel, Mater. Res. Bull. **50**, 417 (2014)
22. J. Zhong, J. Li, F. Feng, Y. Lu, J. Zeng, W. Hu, Z. Tang, J. Mol. Catal. A: Chem. **357**, 101 (2012)
23. M. Shamshi Hassan, M. Shaheer Akhtar, K.-B. Shim, O.-B. Yang, Nanoscale Res. Lett. **5**, 735 (2010)
24. A. Dodd, J. Colloid Interface Sci. **392**, 137 (2013)